Characterization and correction of stray light in optical instruments

Yuqin Zong[a], Steven W. Brown[a], Gerhard Meister[b], Robert A. Barnes[c], and Keith R. Lykke[*a]
[a]National Institute of Standards and Technology, 100 Bureau Drive, Gaithersburg, MD 20899, USA;
[b]Futuretech Corporation, NASA Code 614.2, Goddard Space Flight Center, Greenbelt, MD, USA;
[c]Science Applications International Corporation, 4600 Powder Mill Rd, Beltsville, MD 20705, USA

ABSTRACT

Improperly imaged, or scattered, optical radiation within an instrument is difficult to properly characterize and is often the dominant residual source of measurement error. Scattered light can originate from the spectral components of a "point" source and from spatial elements of an extended source. The spectral and spatial scattered light components are commonly referred to as stray light and can be described by an instrument's spectral line spread function (SLSF) and point spread function (PSF), respectively. In this paper, we present approaches that characterize an instrument's response to scattered light and describe matrices that have been developed to correct an instrument's response for this scattered light. Examples are given to demonstrate the efficacy of the approach and implications for remote sensing instruments are discussed.

Keywords: array detector; astronomy; CCD array; calibration; correction; laser; ocean color; radiometry; remote sensing; spectrograph; spectrometer; spectroradiometer; stray light

1. INTRODUCTION

Stray light within an instrument, both spectral and spatial, is a well-known problem in space-quality remote sensing instruments as well as in commercial instruments. Stray light is mainly caused by scattering from the non-ideal behavior of the optical components (mirrors, slits, grating) and from higher-order diffractions of the grating.

Stray light errors arise when an instrument is used to measure a test source that is quite different, spectrally or spatially, from the calibration source. For example, significant stray light errors may arise when a spectroradiometer is used to measure a narrow band source such as an LED or an LCD since the spectroradiometer is typically calibrated against a Planckian source. Similarly, large radiometric bias errors occur when an imaging radiometer measures moderate to high-contrast structured Earth scenes (e.g. bright clouds over dark oceans and land; broken snow and ice scenes), and thus the measured image needs to be masked for stray light errors and the "contaminated" data needs to be excluded from the final "clean" image product.[1] Xiong, *et al.* found that spectral stray light errors are not negligible in the SWIR band of the Moderate Resolution Imaging Spectroradiometer (MODIS) of the Earth Observing System (EOS) and they developed a linear algorithm to correct the stray light errors caused by the source radiation at a particular wavelength.[2] Spatial stray light is also a problem in MODIS and was studied by Qiu, *et al.*[3] and Meister, *et al.*[4] Du, *et al.* investigated the spatial stray light effect of a commercial CCD camera on the accuracy of the instrument's radiometric calibration and found as large as 3.7 % was introduced by the spatial stray light within the camera.[5]

A number of algorithms have been developed to correct an instrument's imaging characteristics, in both one and two dimensions. One-dimensional algorithms generally correct an instrument's spectral response for scattered light; they are loosely referred to as spectral stray light correction algorithms.[6] In two dimensions, the algorithms are typically used to correct the spatial imaging of instruments such as the Hubble Space Telescope and are referred to as spatial stray light or point-spread response correction algorithms.[3, 7, 8, 9] These previously developed algorithms are generally based on deconvolution approaches that consume a large amount of computing time and are mainly concerned with (and effective with) improving imagery, and focus on sharpening an instrument's response. The algorithms developed for correcting response of the Marine Optical System (MOS) sensor of the NASA's the Marine Optical Buoy (MOBY),[10] both an

*lykke@nist.gov; phone 1 301-975-3216; fax 1 301-975-6991; www.nist.gov

Sensors, Systems, and Next-Generation Satellites XI
edited by Roland Meynart, Steven P. Neeck, Haruhisa Shimoda, Shahid Habib
Proc. of SPIE Vol. 6744, 67441L, (2007) · 0277-786X/07/$18 · doi: 10.1117/12.737315

iterative correction algorithm[11] and a correction matrix,[12, 13, 14] take a different approach. Instead of sharpening an image, these algorithms correct an image only for the small amount of out-of-band (OOB), improperly imaged, or scattered, light within a spectroradiometer's spectral range, or only for the small amount of out-of-field of the resolving power (OOF), improperly imaged, or scattered, light within the imaging radiometer's field-of-view. It is a subtle distinction that has important implications for the stability, robustness, and speed of the algorithms.

We have developed a simple method that is used to correct both spectral and spatial stray light using correction matrices. Part of this method was discussed previously.[12, 13, 14] In this paper, we summarize most of that work, describe new progress, and give two examples of both types of correction. For the spectral stray light correction, we will discuss the MOS unit. For the spatial stray light correction, we will discuss corrections made to a commercial CCD-array imaging radiometer.

2. SPECTRAL STRAY LIGHT CORRECTION

2.1 Characterization of stray light -- development of the Stray-light Distribution Function (SDF) matrix

An instrument's system-level stray light response can be characterized at a particular wavelength by measuring a monochromatic spectral line source to obtain a Spectral Line Spread Function (SLSF). It is critical that the emission of the monochromatic source outside the spectral line is negligible compared to the stray light level of the instrument under test. In general, lasers fulfill this requirement. For proper system-level instrument characterization, it is important that the instrument's entrance pupil be uniformly illuminated.

A SLSF is a spectrograph's relative response to a fixed monochromatic excitation. It is the one-dimensional analog to the point spread function used to describe the two-dimensional spatial imaging characteristics of an instrument. The SLSF for monochromatic radiation centrally imaged on array element J, is denoted $f_{\mathrm{LSF}\ i,\ J}$. The index J is fixed, dependent on the wavelength of the incident radiation; index i runs over all indices in the detector array. For a 512-element detector array, i takes on the discrete values from 1 to 512. For example, Fig. 1 is an SLSF, $f_{\mathrm{LSF}\ i,\ 140}$, normalized by its peak value for convenience.

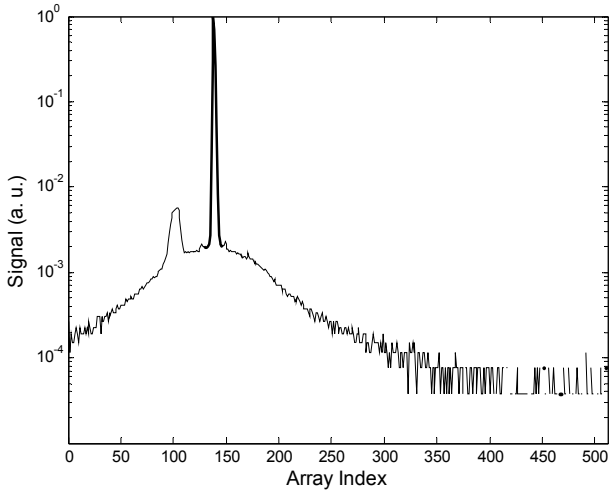

Figure 1. A SLSF for a monochromatic laser excitation centered at array element 140. The dark highlighted region corresponds to the in-band spectral region of the spectrograph.

Dividing the SLSF by the total defined in-band (IB) signal and setting the pixels within the IB area equal to zero gives the relative fractional amount of radiation incident on pixel J that is scattered onto other elements in the detector array. This relative fractional scattering function is called the Stray-light Distribution Function, SDF, denoted $d_{i,J}$, and is shown in Fig. 2 for the SLSF given in Fig. 1.

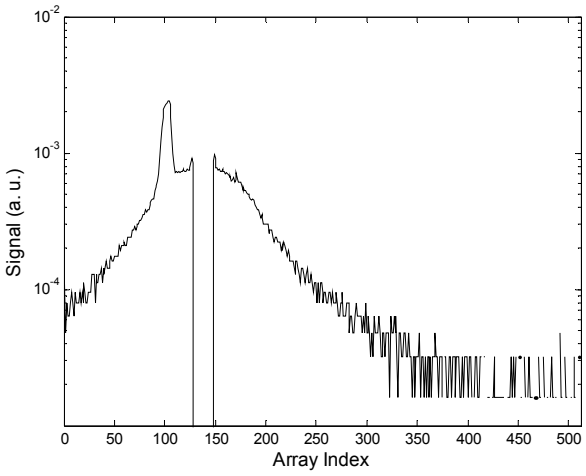

Figure 2. The corresponding SDF to the SLSF shown in Fig. 1.

To fully characterize an instrument's response for spectral stray light, the relative stray light response for every excitation array element J should be known. By tuning the incident laser such that scattering functions can be derived that cover the detector array, an SDF can be developed that describes the full scattering properties of the spectrograph for incident radiation that falls on the array. Incident radiation that does not fall on the array, so-called off-array radiation, is a separate issue and cannot be accounted for by this correction. For optimal results using this approach, off-array radiation should be eliminated through the use of optical blocking filters.

In general, the SDF's of a spectrograph are wavelength dependent; that is, $d_{i,J}$ vary with excitation element J as well as detection element i. It is impractical to directly measure the SDF for every element in the array. However, since the shape of $d_{i,J}$ typically changes smoothly across the array with excitation element J, the $f_{\mathrm{LSF}\ i,\ J}$ can be measured at intervals much larger than the detector element interval, and the $d_{i,J}$ for J between the measured excitation elements can be obtained by interpolation.

With $d_{i,J}$ known for every excitation element J, the spectral scattering properties of the instrument can be fully characterized by a two dimensional, $n \times n$, Stray-light Distribution Function matrix (SDF matrix), **D**, where n is equal to the number of elements in the detector array. **D** is formed by filling the columns of the matrix with the individual SDF's; that is, each column $j = J$ of the matrix **D** is filled with a corresponding $d_{i,J}$ (i = 1 to n). Note that the diagonal elements of the matrix and surrounding elements within the instrument's bandpass are equal to 0 by definition.

$$\mathbf{D} = \begin{bmatrix} d_{1,1} & d_{1,2} \cdots & d_{1,J} \cdots & d_{1,n-1} & d_{1,n} \\ d_{2,1} & d_{2,2} \cdots & d_{2,J} \cdots & d_{2,n-1} & d_{2,n} \\ \vdots & \vdots & \vdots & \vdots & \vdots \\ d_{i,1} & d_{i,2} \cdots & d_{i,J} \cdots & d_{i,n-1} & d_{i,n} \\ \vdots & \vdots & \vdots & \vdots & \vdots \\ d_{n-1,1} & d_{n-1,2} \cdots & d_{n-1,J} \cdots & d_{n-1,n-1} & d_{n-1,n} \\ d_{n,1} & d_{n,2} \cdots & d_{n,J} \cdots & d_{n,n-1} & d_{n,n} \end{bmatrix} \tag{1}$$

While each column corresponds to the relative fractional amount of light hitting other array elements for a particular excitation wavelength, each row I in the matrix forms the relative spectral stray light response function for element $i=I$, $d_{I,j}$ (j = 1 to n). That is, each row I in the matrix gives the relative amount of light scattered onto element i from all other elements j in the array. For a broadband source measurement, the total amount of scattered light falling on element i from all light incident on the detector, $y_{\mathrm{s\_spec},\ i}$, can be expressed as:

$$y_{\text{s\_spec},i} \approx \sum_{j=1}^{n} (d_{i,j} \cdot y_{\text{IB},j}), \tag{2}$$

where $y_{\text{IB},j}$ is the IB signal from element j and the summation extends over all elements in the array.

2.2 Development of the spectral stray-light correction matrix

Consider the measurement equation for detector array element i for the case when a broad-band source is measured. The measured signal from element i, $y_{\text{meas},i}$, is given by

$$y_{\text{meas},i} = y_{\text{IB},i} + y_{\text{s\_spec},i}^{\text{total}}, \tag{3}$$

where $y_{\text{IB},i}$ is the measured IB signal from element i and $y_{\text{s\_spec},i}^{\text{total}}$ is the total signal from element i arising from scattered light. $y_{\text{s\_spec},i}^{\text{total}}$ is the sum of all spectral stray light contributions from the broadband source spectra falling on different elements in the array plus scattered light from all other sources, $\delta_{\text{spec},i}$:

$$y_{\text{s\_spec},i}^{\text{total}} = \sum_{j=1}^{n} (d_{i,j} \cdot y_{\text{IB},j}) + \delta_{\text{spec},i} \tag{4}$$

In particular, $\delta_{\text{spec},i}$ includes contributions from off-array scattered light. This is scattered light that is never imaged onto the detector array. There is a detected signal from this light because in most cases, the spectrum of a measured broad-band source extends beyond an instrument's designed spectral coverage range; in addition, the spectral response of the detectors used is typically broader than the designed spectral range. As previously stated, $\delta_{\text{spec},i}$ cannot be quantified and corrected with the method being described; however, this component may be negligible, or can be reduced to a negligible level by properly filtering the radiation entering the spectrograph, or can be estimated for a particular source by using a proper optical filter. Setting $\delta_{\text{spec},i}$ equal to zero, Eq. 3 can be written as:

$$y_{\text{meas},i} = y_{\text{IB},i} + \sum_{j=1}^{n} (d_{i,j} \cdot y_{\text{IB},j}) \ . \tag{5}$$

Considering all elements in the array, Eq. 5 can be expressed in matrix form,

$$\mathbf{Y}_{\text{meas}} = \mathbf{Y}_{\text{IB}} + \mathbf{D} \cdot \mathbf{Y}_{\text{IB}}, \tag{6}$$

where $\mathbf{Y}_{\text{meas}}$ is a column vector comprised of the n measured signals from the detector array and $\mathbf{Y}_{\text{IB}}$ is a column vector representing the IB signals from the n array elements.

Equation 6 can be rewritten as:

$$\mathbf{Y}_{\text{meas}} = [\mathbf{I} + \mathbf{D}] \cdot \mathbf{Y}_{\text{IB}} = \mathbf{A} \cdot \mathbf{Y}_{\text{IB}}, \tag{7}$$

where $\mathbf{A}$ (=$\mathbf{I}$+$\mathbf{D}$) is a square coefficient matrix of order n and $\mathbf{I}$ is the $n \times n$ identity matrix. $\mathbf{A}$ has a particular form, with the in-band area of each element compressed into a single element along the matrix diagonal. The adjacent elements, those corresponding to the in-band area, are set equal to 0, and the other elements in the array are all much less than 1.

In Eq. 5, there are a total of n equations, and the n $y_{\text{IB},i}$ are the unknown quantities of interest. The matrix measurement equation, Eq. 6, as well as Eq. 7, are systems of simultaneous linear equations that have the same number of equations as unknowns (n). Each unknown column vector $\mathbf{Y}_{\text{IB}}$ can be obtained by directly solving Eq. 7 using a proper linear algebraic algorithm (*e.g.* the Gaussian elimination algorithm). However, in terms of simplicity and calculation speed, it is preferable to solve Eq. 7 by inverting matrix $\mathbf{A}$:

$$\mathbf{Y}_{\text{IB}} = \mathbf{A}^{-1} \cdot \mathbf{Y}_{\text{IB}} = \mathbf{C}_{\text{spec}} \cdot \mathbf{Y}_{\text{meas}}. \tag{8}$$

$\mathbf{C}_{\text{spec}}$, the inverse of $\mathbf{A}$, is called the spectral stray light correction matrix. Using Eq. 8, the spectral stray light correction becomes a single matrix multiplication operation, and the correction can be performed in real-time with minimal impact

on acquisition speed. Note that development of matrix $\mathbf{C}_{spec}$, as with the development of matrix **D**, is required only once, unless the imaging or scattering characteristics of the instrument change.

2.3 Example of spectral stray light correction: MOS ROV system

The Marine Optical System Remotely Operated Vehicle (MOS ROV)[17] system was characterized for stray light properties on the NIST SIRCUS facility [15, 16, 18]. The MOS ROV is a fiber-coupled dual-spectrograph system covering the spectral range from 340 nm to 955 nm. The scattering characteristics of the MOS ROV were determined using tunable lasers on SIRCUS that covered the full MOS ROV spectral range.. The lasers were introduced into a 30 cm diameter integrating sphere with a 7.5 cm diameter exit port. The MOS ROV fiber input was centered on the exit port, ensuring that the entrance pupil of the MOS system was over-filled.

Shown in Fig. 3 is an image of the slit on the CCD from a monochromatic laser source and the relative signal from the CCD array averaged over the rectangle shown in the left hand figure. The right-hand side of Fig. 3 shows the intense central peak, which is the properly imaged entrance slit. The figure also contains a broad, haze-like component and a non-zero diffuse component to the image. These two components are the scattered light signal from the image. The spectral stray light correction algorithm corrects a measured spectral radiance for this scattered light.

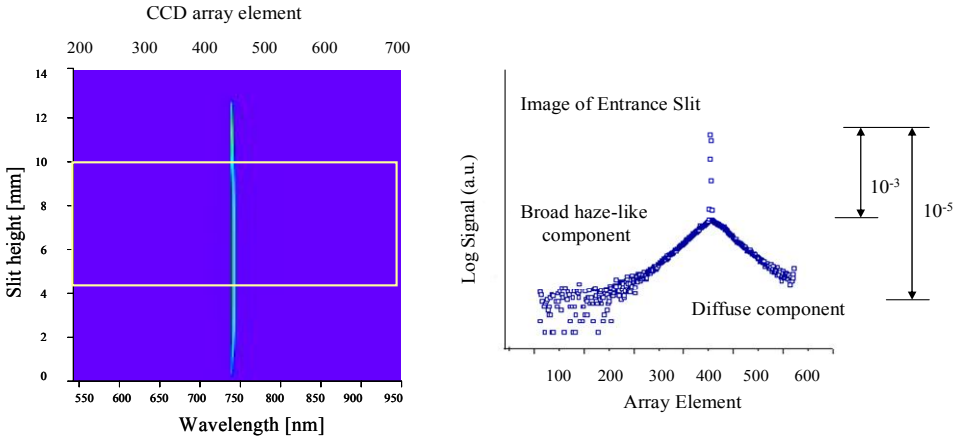

Figure 3. The image of the slit on the CCD from a monochromatic laser source and the relative signal from the CCD array.

For MOS, any spatial information of the sources being measured within its field-of-view is ignored. That is, MOS measures the average spectral radiance of the source being measured, either a calibration source or up-welling radiance in the ocean. In this case, the output of the spectrograph, which uses a two dimensional array detector, is integrated along a column, giving a one-dimensional response. A one-dimensional spectral stray light response correction matrix is used to correct MOS for scattered light.

A set of representative SLSFs are shown in Fig. 4 for the ROV blue spectrograph. The IB area is highlighted for each wavelength. A total of 80 laser lines were measured, ensuring adequate coverage to properly characterize rapidly changing features such as the spurious reflection peak. Only the relative spectral distribution as a function of array element is required for the stray light correction. The wavelength scale for the spectrograph is given on the top axis of the figure. Because of the 0.01 nm wavelength uncertainty on the SIRCUS facility, these data can be used to provide an accurate wavelength calibration of the spectrograph.

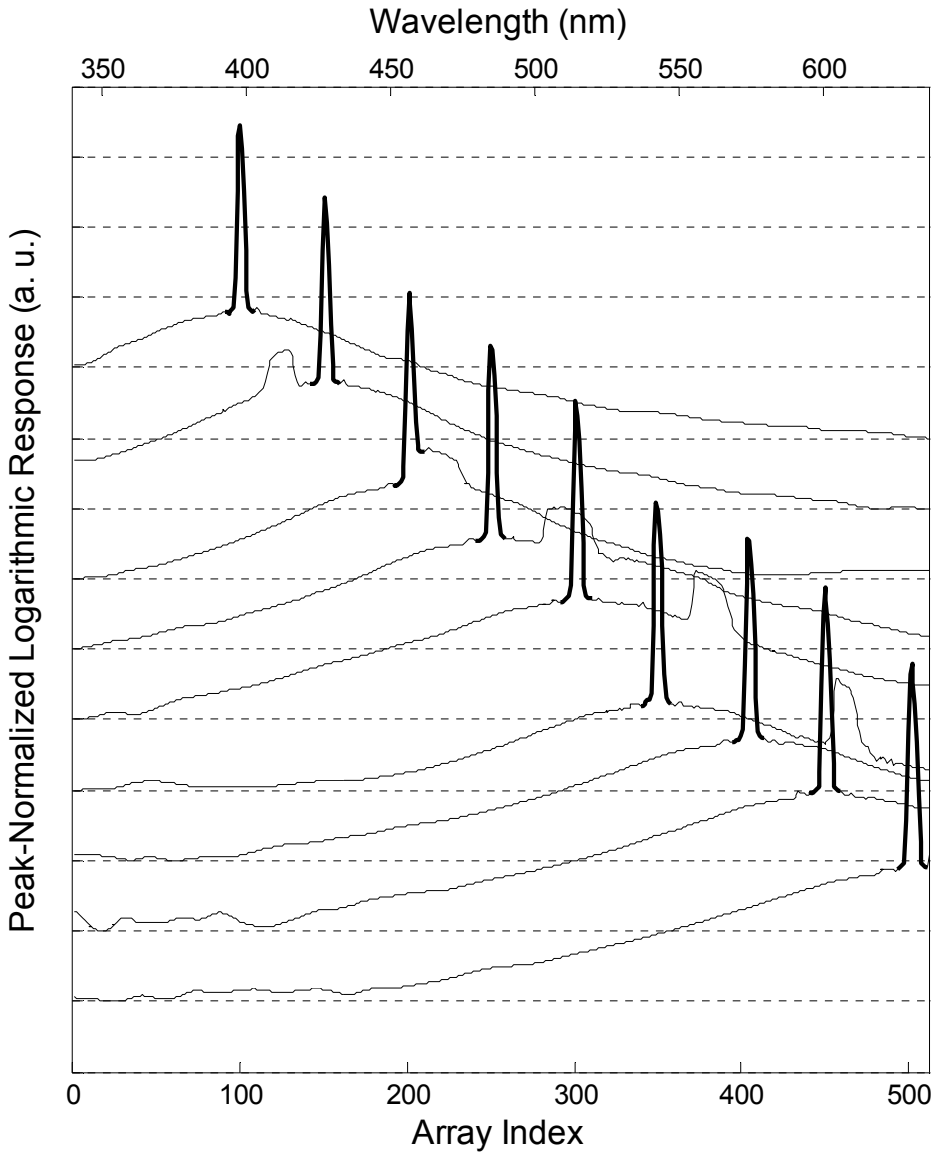

Figure 4. Representative SLSFs of the MOS ROV blue spectrograph. The IB region of each SLSF is highlighted in black..

Normalizing the laser characterization data by the total IB signal and setting the in-band pixels in each set of laser data to 0, the $d_{i,J}$ for J =100, 200, 300, 400, and 500 are shown in Fig. 5. A partial D-matrix formed from the $d_{i,J}$ is shown in Fig. 6 while the full D-matrices for the blue spectrograph is shown in Fig. 7. The full matrices were formed by linearly interpolating the laser line data to fill in the intervening matrix elements. Note that the center pixels have been given a nominal value of $1e^{-6}$ instead of zero for these logarithmic graphs.

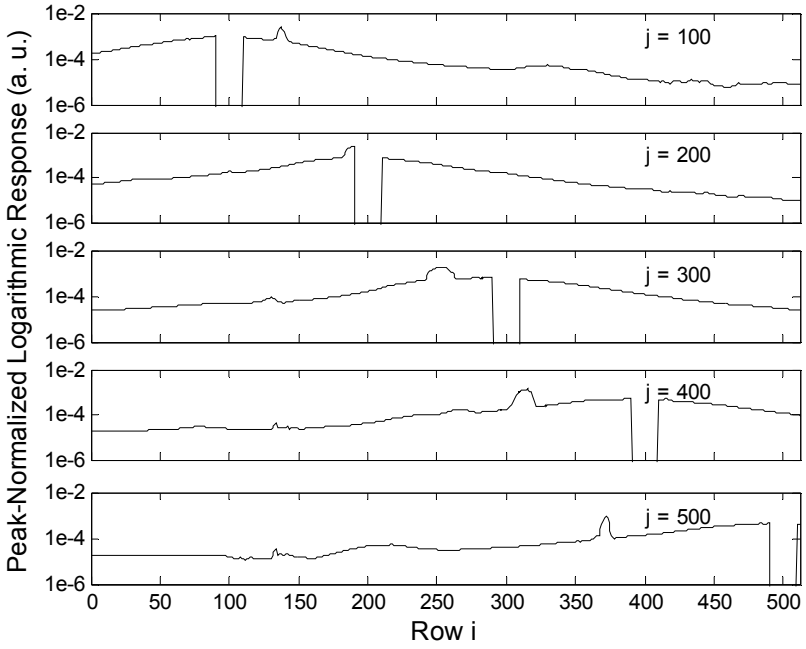

Figure 5. MOS ROV SDFs for J=100, 200, 300, 400, and 500 for the blue spectrograph.

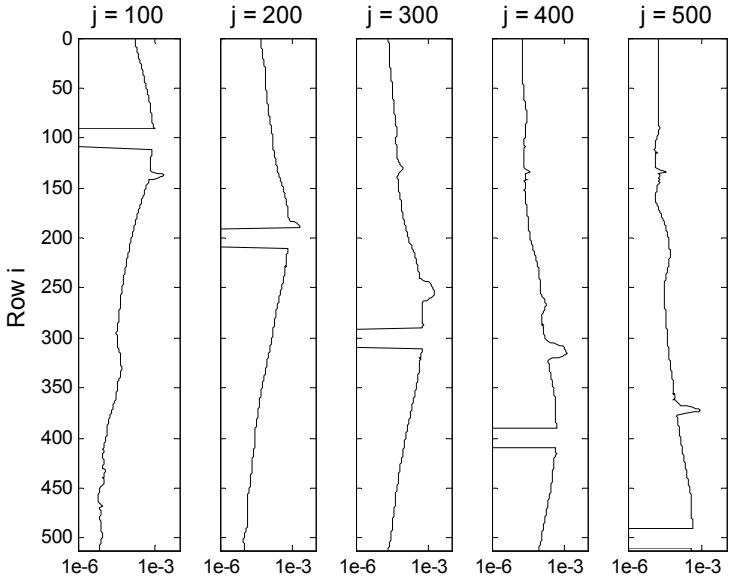

Figure 6. MOS ROV partial D-matrix formed from the $d_{i,J}$ shown in Fig. 5 for the blue spectrograph.

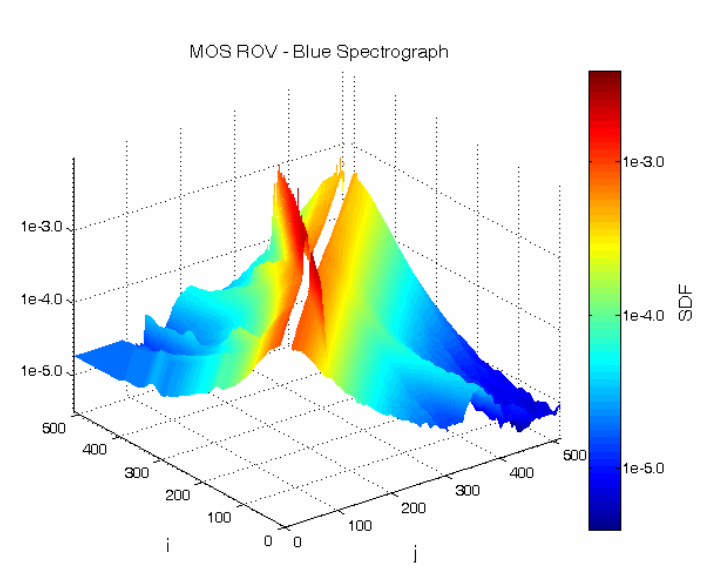

Figure 7. MOS ROV full D-matrix for the blue spectrograph.

The stray light correction matrix **C** for the spectrograph has been validated. Figure 8 shows the results of the ROV blue spectrograph for the measurement of a blue LED diver lamp. For this LED, no radiation is expected outside of the primary peak. The figure illustrates that, by applying stray light correction matrix to the data, the errors outside of this region are reduced by more than one order of magnitude.

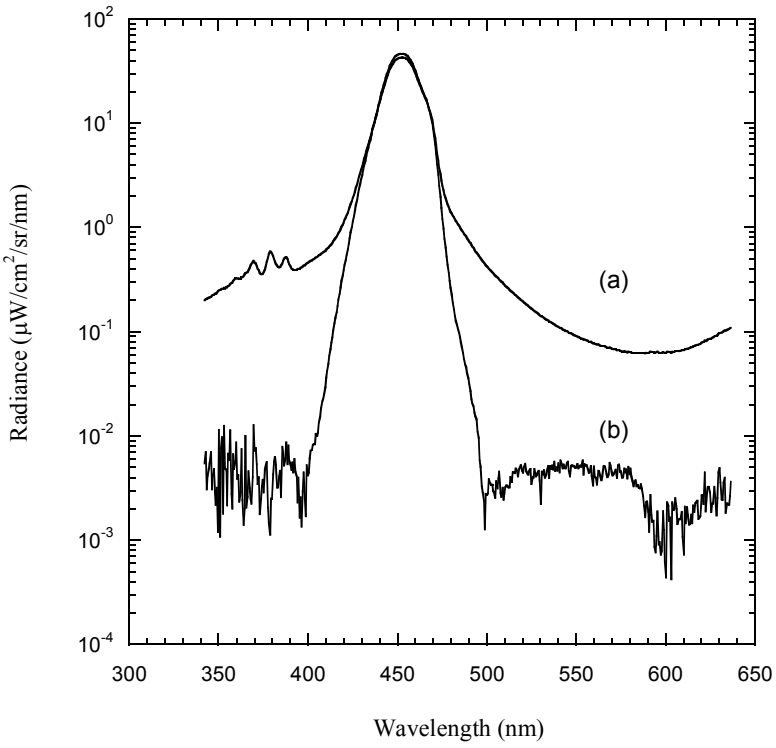

Figure 8. Results of the stray light correction: (a) raw ($\mathbf{Y}_{meas}$) and (b) stray light corrected ($\mathbf{Y}_{IB}$) MOS ROV signals for the measurement of a blue LED diver lamp.

3. SPATIAL STRAY LIGHT CORRECTION

3.1 Development of the spatial stray-light correction matrix

For spatial stray-light correction, an imaging instrument is first characterized for a set of point-spread functions (PSFs) covering the imaging instrument's field-of-view. A PSF is a 2-dimensional relative spatial response of an imaging instrument when it is used to measure a point source (or a small pin-hole source). Each PSF is used to derive an SDF: the ratio of the stray-light signal to the total signal within the field of resolving power of the imaging instrument. By using the set of derived SDFs and interpolating between these SDFs, all SDFs are obtained. Each of the obtained 2-dimensional SDFs is transformed to a 1-dimensional column vector. By using all of the column vector SDFs, a SDF matrix is obtained. Similar to the spectral stray-light correction, the SDF matrix is then used to derive the spatial stray-light correction matrix, and the instrument's response to stray light is corrected by

$$\mathbf{Y}_{IF} = \mathbf{C}_{spat}\mathbf{Y}_{meas} \tag{9}$$

where $\mathbf{C}_{spat}$ is the spatial stray-light correction matrix, $\mathbf{Y}_{meas}$ is the column vector of the measured raw signals obtained by transforming 2-dimensional imaging signals, and $\mathbf{Y}_{IF}$ is the column vector of the spatial stray-light corrected signals. Note that, as with the spectral stray light correction algorithm, development of matrix $\mathbf{C}_{spat}$ is required only once, unless the imaging characteristics of the instrument changes. Using Eq. 9, the spatial stray-light correction also becomes a single matrix multiplication. Note that the measured PSFs also include other types of unwanted response from the imaging instrument (e.g., CCD smearing); the stray-light correction eliminates these types of errors as well.

3.2 Example of spatial stray light correction: a commercial CCD-array imaging radiometer

A commercial CCD-array imaging radiometer was corrected for spatial stray light. The focal length of the imaging radiometer is 55 mm and the detector of the imaging radiometer is a room temperature, progressive scan CCD with an electronic shutter. The total number of elements is 1.4 million, and the resolution of the A/D converter is12-bit. Figure 9 shows the measured PSF for a 0.2 mm pinhole on an integrating sphere port with the camera imaging the pinhole from a distance of 2 m. As with spectral scattered light, there is a strong central peak along with diffuse wings.

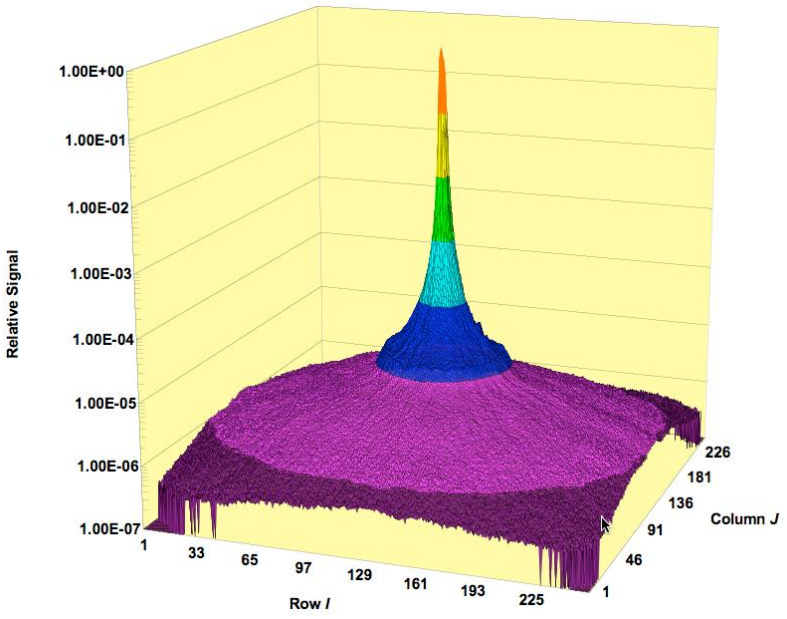

Fig. 9. A measured point-spread function of the CCD-array imaging radiometer.

The spatial stray-light corrected imaging radiometer was used to measure radiance on the port of an integrating sphere source. The size of the sphere port was adjusted to be smaller than the field-of-view of the imaging radiometer, so that the spatial stray-light signals arising from the source outside the field-of-view of the imaging radiometer were theoretically zero. Figure 10 shows the results of correction for a white spot (the sphere port) measurement and a black spot (a small piece of black aluminum foil hung at the center of the sphere port) measurement, which are logarithmic and linear plots of 1-dimensional signals along a center line across the sphere port. The maximum signal (not plotted) is normalized to one. It is clear that in the case of measurement of the black spot, the level of spatial stray light of the imaging radiometer is approximately 10^{-2} and it is reduced by more than one order of magnitude after the spatial stray-light correction.

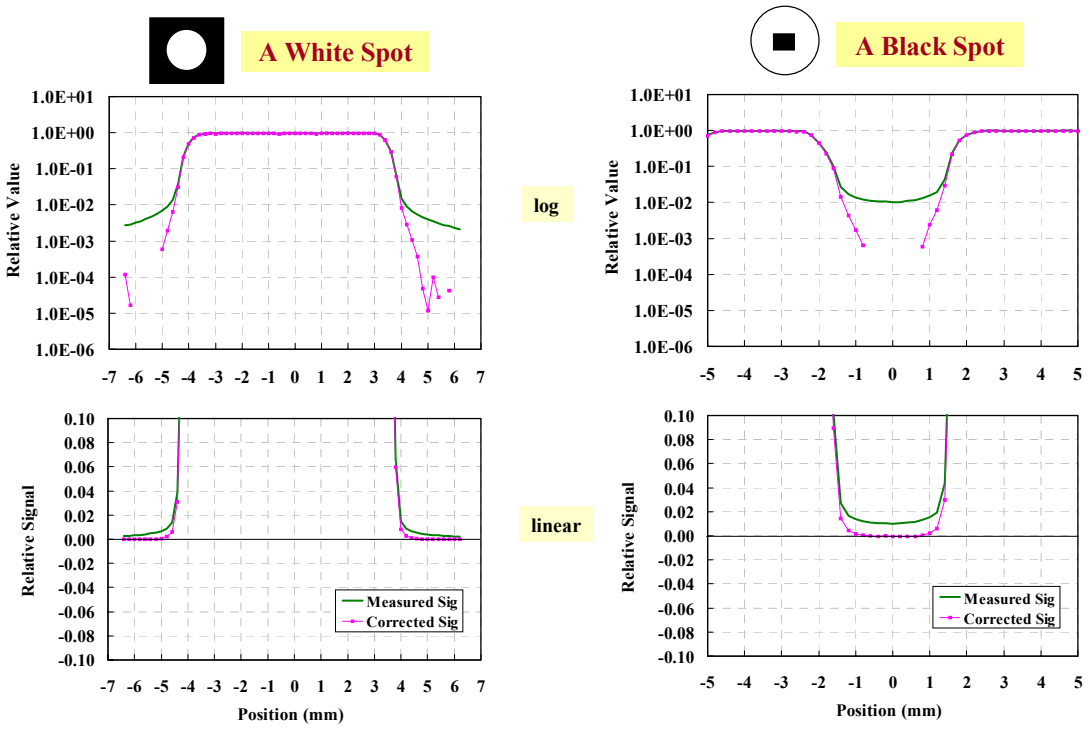

Figure 10. Results of spatial stray-light correction.

4. SUMMARY

In this paper, we have presented approaches that characterize an instrument's response to scattered light and have described matrices that have been developed to correct an instrument's response to this scattered light. Examples for both spectral and spatial stray light corrections have been given to demonstrate the efficacy of this method. These algorithms, applied to satellite sensors, could significantly reduce out-of-band systematic errors as well as errors arising from bright targets in a scene, for example the case where there is a bright cloud in an otherwise dark ocean color image. However, the efficacies of the algorithms are predicated on accurate laboratory system-level characterization prior to launch. In fact, no algorithm can work well without adequate pre-launch system-level characterization of the sensor, This re-emphasizes the axiom that pre-launch characterization is as important as pre-launch calibration for optimal on-orbit sensor performance.

ACKNOWLEDGMENTS

The authors thank Jack Xiong at NASA, B. Carol Johnson at NIST, Stephanie Flora at Moss Landing Marine Laboratories, and Dennis Clark at Marine Optical Consulting for helpful discussions regarding stray light in remote sensing instruments.

REFERENCES

[1] B. Franz and G. Meister, http://oceancolor.gsfc.nasa.gov/REPROCESSING/Aqua/R1/modisa_repro1_stlight.html

[2] X. Xiong X., K. Chiang, F. Adimi, W. Li, H. Yatagai, AND W.L. Barnes, "MODIS Correction Algorithm for out-of-band Response in the Short-wave IR Bands, " Proc. SPIE **5234**, 605–613 (2004).

[3] S. Qiu, G. Godden, X. Wang, AND B. Guenther, "Satellite-Earth Remote Sensor Scatter Effects on Earth Scene Radiometric Accuracy, " Metrologia **37**, 411–414 (2000).

[4] G. Meister, B. A. Franz, K. Turpie, and C. R. McClain, "The MODIS Aqua Point-Spread Function for Ocean Color Bands," ISPRS **36**, 7/W20, (2005).

[5] D. Hong and K. J. Voss, "Effects of point-spread function on calibration and radiometric accuracy of CCD camera," Appl. Opt., **43**, 665–670 (2004).

[6] H. J. Kostkowski, Reliable Spectroradiometry, (Spectroradiometry Consulting, La Plata, MD), 1997, Chapter 4.

[7] S. M. Jefferies and J. C. Christou, "Restoration of astronomical images by iterative blind deconvolution," The Astrophysical Journal, **415**, 862-874 (1993).

[8] W. C. Keel, "A simple, photometrically accurate algorithm for deconvolution of optical images," Publications of the Astronomical Society of the Pacific, **103** 723–729 (1991).

[9] H. Li, M. S. Robinson, and S. Murchie, "Preliminary remediation of scattered light in NEAR MSI images," Icarus **155**, 244–252 (2002).

[10] C. Habauzit, S. W. Brown, K. R. Lykke, B. C. Johnson, M. E. Feinholz, M. Yarbrough, and D. K. Clark, "Radiometric Characterization and Absolute Calibration of the Marine Optical System (MOS) Bench Unit," J. Atmos. Oceanic Technol. **20**, 383–391, (2003).

[11] S. W. Brown, B. C. Johnson, M. E. Feinholz, M. A. Yarborough, S. J. Flora, K. R. Lykke, and D. K. Clark, "Stray-light correction algorithm for spectrographs," Metrologia, **40**, S81–S84 (2003).

[12] Y. Zong, S. W. Brown, B. C. Johnson, K. R. Lykke, and Y. Ohno, "Correction of stray light in spectrographs: implications for remote sensing," Proc. SPIE **5882**, 1–8, (2005)

[13] Y. Zong, S. W. Brown, B. C. Johnson, K. R. Lykke, and Y. Ohno, "Simple spectral stray light correction method for array spectrometers," Appl. Opt. **45**, 1111–1119 (2006).

[14] Y. Zong, S. W. Brown, B. C. Johnson, K. R. Lykke, and Y. Ohno, "Correction of stray light in spectroradiometers and imaging instruments, " Proc. CIE, **CIE 178**, D2-33–D2-36 (2007).

[15] S. W. Brown, G. P. Eppeldauer, and K. R. Lykke, "Facility for spectral irradiance and radiance responsivity calibrations using uniform sources," Appl. Opt. **40**, 8218–8237 (2006).

[16] S. W. Brown, G. P. Eppeldauer, and K. R. Lykke, "NIST facility for Spectral Irradiance and Radiance Responsivity Calibrations with Uniform Sources," Metrologia, **37**, 579–582 (2000).

[17] M. A. Yarbrough, *et al*., "Results in coastal waters with high resolution in situ spectral radiometry: The Marine Optical System ROV," Proc. SPIE **6680**, 6680-15 (2007), in press.

[18] M. E. Feinholz, *et al*., "Stray light correction of the Marine Optical System," submitted for publication to J. Atmos. Oceanic Technol.